

## The $M_{\text{BH}}-R_{\text{b}}$ relation and the high-mass end of the $M_{\text{BH}}-\sigma$ relation

BILILIGN T. DULLO <sup>1</sup>

<sup>1</sup>*Embry-Riddle Aeronautical University, Daytona Beach, FL 32114, USA*

### ABSTRACT

Using a sample of 151 galaxies with dynamically measured black hole (BH) masses ( $M_{\text{BH}}$ ), we investigate the scaling relations between  $M_{\text{BH}}$  and the stellar velocity dispersion,  $\sigma$ , and, for a subsample of 30 core-Sérsic galaxies, between  $M_{\text{BH}}$  and the size of the partially depleted core,  $R_{\text{b}}$ . Core-Sérsic galaxies, identified using high-resolution *Hubble Space Telescope* imaging and spanning both the normal-core ( $R_{\text{b}} < 0.5$  kpc) and large-core ( $R_{\text{b}} > 0.5$  kpc) regimes, define an updated  $M_{\text{BH}}-R_{\text{b}}$  relation of the form  $M_{\text{BH}} \propto R_{\text{b}}^{1.16 \pm 0.10}$ , with an rms scatter of  $\Delta_{\text{rms}} \simeq 0.28$  dex in  $\log M_{\text{BH}}$ . We find that Sérsic and normal-core galaxies together follow a common log-linear  $M_{\text{BH}}-\sigma$  relation with a slope of  $4.95 \pm 0.29$  and a scatter  $\Delta_{\text{rms}} \simeq 0.46$  dex. Deviations from this relation arise at the highest BH masses, where large-core galaxies, including six with direct  $M_{\text{BH}}$  measurements, drive a significant upturn. We find that these galaxies typically host ultramassive black holes whose masses scale more strongly with  $R_{\text{b}}$  than  $\sigma$ , and lie  $\sim (1-4)\times$  the intrinsic scatter (0.39 dex) above the relation defined by Sérsic and normal-core galaxies. The  $M_{\text{BH}}-R_{\text{b}}$  relation shows  $\sim 30-47\%$  less scatter in  $\log M_{\text{BH}}$  than the corresponding  $M_{\text{BH}}-\sigma$  relation for the same sample. We interpret the high-mass upturn in the  $M_{\text{BH}}-\sigma$  diagram as a consequence of successive major, dry mergers, a scenario that naturally explains the observed flattening of the  $\sigma - L_V$  relation at  $M_V \lesssim -23.5$  mag.

*Keywords:* Supermassive black holes (1663) — cD galaxies (209) — Elliptical galaxies (456) — Lenticular galaxies (915) — Galaxy photometry (611) — Galaxy nuclei (609) — Galaxy structure (622)

### 1. INTRODUCTION

Observations have shown that all massive elliptical galaxies and massive bulges of disk galaxies host central black holes (BHs) with masses  $M_{\text{BH}} \sim 10^6 - 10^{10} M_{\odot}$  (Kormendy & Richstone 1995; Magorrian et al. 1998; Ferrarese & Ford 2005). The masses of such black holes are known to correlate with several host galaxy properties, including: stellar velocity dispersion,  $\sigma$  (Ferrarese & Merritt 2000; Gebhardt et al. 2000; McConnell & Ma 2013), spheroid luminosity,  $L$  (e.g., Kormendy & Richstone 1995; McLure & Dunlop 2002), dynamical mass (e.g., Magorrian et al. 1998; Marconi & Hunt 2003; Häring & Rix 2004) and galaxy UV-[3.6] color (Dullo et al. 2020).

In the standard cosmological paradigm, galaxies grow hierarchically through the merger of smaller systems (White & Rees 1978; White & Frenk 1991; Khochfar & Burkert 2001). The ubiquity of central supermas-

sive black holes (SMBHs)—combined with the rarity of binary SMBHs—suggests that progenitor black holes have coalesced in most merged galaxies. During major dry (dissipationless) mergers, inspiralling SMBH binaries transfer orbital angular momentum to surrounding stars, ejecting them from the central regions and producing partially depleted stellar cores in luminous ( $M_V \lesssim -21.50 \pm 0.75$  mag) core-Sérsic galaxies (e.g., Begelman et al. 1980; Ebisuzaki et al. 1991; Milosavljević & Merritt 2001; Merritt 2006; Gualandris & Merritt 2012; Khan et al. 2013; Vasiliev et al. 2015; Rantala et al. 2018; Nasim et al. 2020). Consistent with this picture, careful modeling of core-Sérsic galaxies using HST imaging have revealed a strong correlation between black hole mass and the size of depleted cores, as measured by the break radius,  $R_{\text{b}}$  (e.g., Lauer et al. 2007; Dullo & Graham 2012, 2014; Dullo 2019; Dullo et al. 2021).

The tight  $M_{\text{BH}}-R_{\text{b}}$  relation, which holds across the full mass range of core-Sérsic spheroids, has been largely overlooked, despite displaying a lower level of scatter than the  $M_{\text{BH}}-\sigma$  relation (Dullo 2019; Dullo et al.

2021). The  $M_{\text{BH}} - \sigma$  relation (e.g., van den Bosch 2016), which exhibits an upturn at the high mass end, predicts that SMBH masses in the most massive galaxies (i.e.,  $\sigma \sim 300 - 390 \text{ km s}^{-1}$ , Sheth et al. 2003; Lauer et al. 2007; Bernardi et al. 2007; Lauer et al. 2014) cannot exceed  $M_{\text{BH}} \sim 6 \times 10^9 M_{\odot}$ . However, ultramassive black holes (UMBHs;  $M_{\text{BH}} \gtrsim 10^{10} M_{\odot}$ ) are increasingly discovered at the centers of extremely massive present-day galaxies (e.g., McConnell et al. 2011; Thomas et al. 2016; Mehrgan et al. 2019; Surti et al. 2024; de Nicola et al. 2024). Dullo et al. (2021) found that the  $M_{\text{BH}} - \sigma$  relation underestimates the black hole mass for the most massive galaxies by up to a factor of 40 (see also Dullo 2019). Furthermore, predicted  $M_{\text{BH}}$  from the  $M_{\text{BH}} - R_{\text{b}}$  and  $M_{\text{BH}} - L$  relations can exceed  $10^{10} M_{\odot}$  (Lauer et al. 2007; Dullo 2019; Dullo et al. 2021).

The upturn of the  $M_{\text{BH}} - \sigma$  relation at the highest  $\sigma$  is consistent with substructure observed in the well-known Faber & Jackson (1976,  $\sigma \propto L^{1/4}$ ) relation for core-Sérsic galaxies. Dullo (2019) separated core-Sérsic galaxies into normal-core ( $R_{\text{b}} < 0.5 \text{ kpc}$ ) and large-core ( $R_{\text{b}} \gtrsim 0.5 \text{ kpc}$ ) galaxies. They found that the  $\sigma - L_V$  relation flattens and exhibits larger scatter for large-core spheroids with  $M_V \lesssim -23.50 \pm 0.10 \text{ mag}$ ,  $M_* \gtrsim 10^{12} M_{\odot}$  and  $R_e \gtrsim 10 \text{ kpc}$  (see also Oegerle & Hoessel 1991; Boylan-Kolchin et al. 2006; Lauer et al. 2007; Hlavacek-Larrondo et al. 2012; Mezcua et al. 2018; Dullo 2019; Dullo et al. 2021; Sasseville et al. 2025). For the combined sample of normal- and large-core galaxies, the slope of the  $\sigma - L$  relation,  $1/(5.00 \pm 0.63)$ , is shallower than that of normal-core spheroids alone,  $1/(3.50 \pm 0.61)$ ; see also Malumuth & Kirshner 1981; Lauer et al. 2007; Kormendy & Bender 2013). At lower luminosities ( $M_V \gtrsim -21.5 \text{ mag}$ ), coreless Sérsic galaxies follow a steeper relation,  $\sigma \propto L^{1/2}$  (e.g., Held et al. 1992; Matković & Guzmán 2005).

In a continued effort to investigate the  $M_{\text{BH}} - R_{\text{b}}$  relation, and the offset at the high-mass end of the  $M_{\text{BH}} - \sigma$  relation, we expand the sample of core-Sérsic galaxies with dynamically measured black hole masses presented in Dullo et al. (2021) by  $\sim 25\%$ . Our full sample of 79 core-Sérsic galaxies represents the largest to date used to study the  $M_{\text{BH}} - R_{\text{b}}$  and  $M_{\text{BH}} - \sigma$  relations for core-Sérsic galaxies.

Section 2 discusses our sample of 151 galaxies with dynamically measured SMBH masses, coupled with the 49 core-Sérsic galaxies with predicted  $M_{\text{BH}}$ . Section 3 discusses the linear regression methods adopted. In Section 4.1, we compare the strengths of the  $M_{\text{BH}} - R_{\text{b}}$  and core-Sérsic  $M_{\text{BH}} - \sigma$  relations. Dividing our sample into Sérsic, normal-core and large-core galaxies, in Sections 4.2 and 4.3 we reveal substructure in the  $M_{\text{BH}} - \sigma$

diagram. In Section 4.4, we present  $M_{\text{BH}}$  predicted using the  $M_{\text{BH}} - \sigma$  and  $M_{\text{BH}} - L$  relations and discuss underestimated BH masses of large-core galaxies in the  $R_{\text{b}} - M_{\text{BH}}$  diagram. Section 5 discusses the dry merger scenario that has been presented in the literature to explain the upturn at the high-mass end of the  $M_{\text{BH}} - \sigma$  relation. In Section 6, we summarize our main conclusions. We include an appendix at the end of this paper presenting the BH scaling relations derived from our forward BCES and LINMIX (Y|X) regression fits.

## 2. SAMPLE AND DATA

We note that most of the data used in this work to study the BH scaling relations are published elsewhere (Dullo & Graham 2014; Dullo 2019; Dullo et al. 2021, 2023a).

To identify the partially depleted cores for the large-core and normal-core galaxies, we fitted the core-Sérsic model to the *HST* stellar light distributions of the spheroidal components of the galaxies (Dullo & Graham 2014, 2015; Dullo 2019; Dullo et al. 2021, 2023a,b, 2024).

Using a sample of 24 core-Sérsic galaxies with directly measured SMBH masses and 27 core-Sérsic with predicted SMBH masses, Dullo et al. (2021) investigated the  $M_{\text{BH}} - R_{\text{b}}$  relation, and the offset at the high-mass end of the  $M_{\text{BH}} - \sigma$  relation. Here, we expand the sample of core-Sérsic galaxies with direct SMBH masses from 24 to 30, representing a 25% increase, and increase the number of core-Sérsic galaxies with predicted SMBH masses from 27 to 49, an  $\sim 82\%$  increase (Tables 1 and 2). Our full sample of 79 core-Sérsic galaxies are compiled by combining the data from Dullo & Graham (2014), Dullo (2019) Dullo et al. (2023a) and 13 core-Sérsic galaxies in this work (Table 2). Of the 30 (49) core-Sérsic galaxies with directly measured (predicted) SMBH masses, three (14) have large cores (i.e.,  $R_{\text{b}} > 0.5 \text{ kpc}$ ).

We also present the  $M_{\text{BH}} - R_{\text{b}}$  and  $M_{\text{BH}} - \sigma$  relations, including three galaxies recently reported to host large cores and ultramassive black holes: 4C+37.11 (Surti et al. 2024), Holm 15A (Mehrgan et al. 2019), and NGC 708 (de Nicola et al. 2024). Core-Sérsic galaxies possess a central stellar light (or mass) deficit relative to the inward extrapolation of their outer Sérsic (1963, 1968)  $R^{1/n}$  profile, resulting in shallow inner slopes ( $\gamma \lesssim 0.3$ ). However, Holm 15A and NGC 708 were not identified as having such deficits (Mehrgan et al. 2019; de Nicola et al. 2024), while 4C+37.11 was modeled with a core-Sérsic model with a sharper transition ( $\alpha = 100$ ) and a relatively steep inner slope,  $\gamma \sim 0.44$ , (Surti et al. 2024).

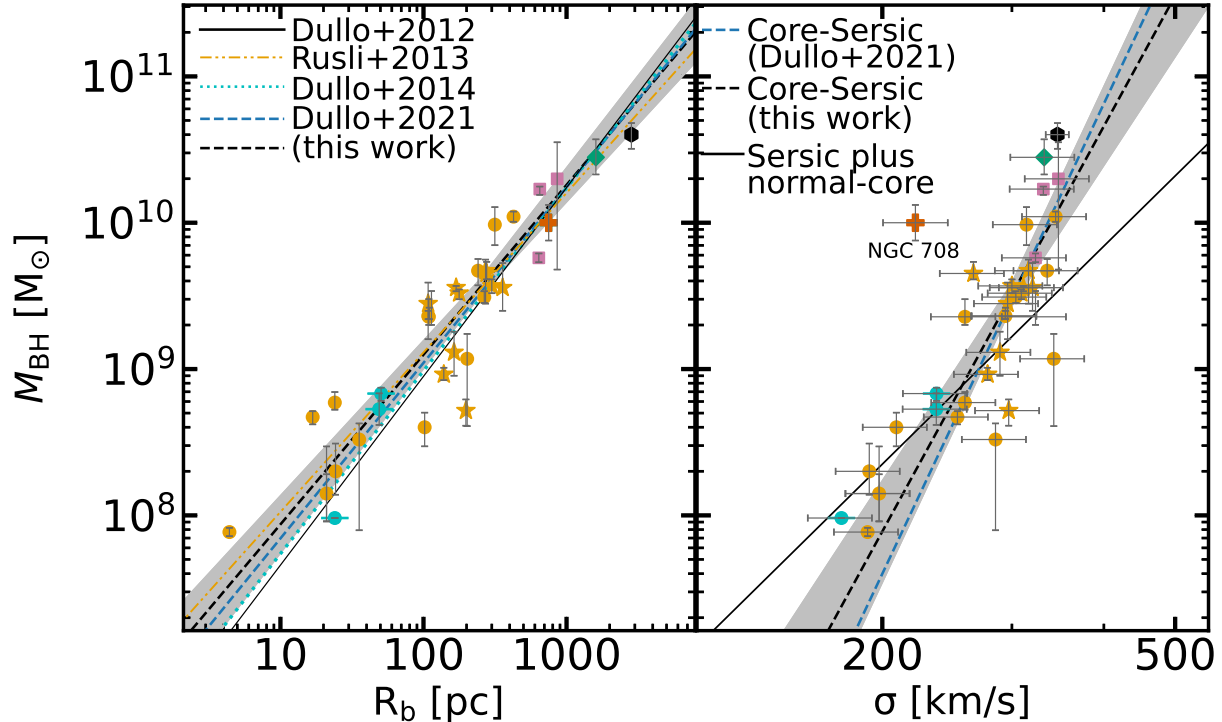


**Figure 1.** Relation between SMBH mass ( $M_{\text{BH}}$ ) and (a) the core-Sérsic break radius ( $R_b$ ) and (b) central velocity dispersion ( $\sigma$ ) for a sample of 30 core-Sérsic galaxies with dynamically determined  $M_{\text{BH}}$ . The black dashed lines are our symmetric BCES bisector regression fits (Table 4). Filled orange circles and cyan disk symbol represent the 14 normal-core (i.e.,  $R_b < 0.5$  kpc) elliptical galaxies and the three normal-core lenticular (S0) galaxies from Dullo & Graham (2014, their Table 2), respectively, while filled purple boxes denote the three large-core (i.e.,  $R_b > 0.5$  kpc) elliptical galaxies from Dullo (2019). The 10 normal-core elliptical galaxies from Rusli et al. (2013a) are indicated by filled orange stars. The shaded regions show the  $1\sigma$  uncertainty for the regression fits (black dashed lines). While we show the uncertainties on  $R_b$ , they are smaller than the symbol sizes. The dash-dot-dot line (left panel) represents the  $M_{\text{BH}} - R_b$  relation from Rusli et al. (2013a). The black solid line (right panel) shows the symmetric BCES bisector fit to our Sérsic + normal-core sample with dynamically determined  $M_{\text{BH}}$ . Including 4C+37.11 (diamond, Surti et al. 2024), Holm 15A (hexagon, Mehrgan et al. 2019), and NGC 708 (cross, de Nicola et al. 2024)—excluded from our primary sample of 30 core-Sérsic galaxies (see the text for details)—does not change the  $M_{\text{BH}} - R_b$  relation.

For Holm 15A, Mehrgan et al. (2019) reported the so-called ‘cusp radius’, defined as the radius where the local logarithmic slope  $\gamma = 1/2$  (Carollo et al. 1997). We note that even galaxies without depleted cores can have a radius at which  $\gamma = 1/2$ . For NGC 708, de Nicola et al. (2024) fitted the inner part of the spheroid using a core-Sérsic model with a low Sérsic index ( $n \sim 1.8$ ) and a small effective radius  $R_e \sim 0.5$  kpc. However, the break radius is known to be sensitive to the adopted fitted range, particularly when the light profile does not cover the full radial extent of the spheroid (Dullo & Graham 2012).

Nevertheless, using HyperLeda photometric and kinematic measurements, we find that all three galaxies fulfill the criteria commonly associated with core-Sérsic galaxies, namely high luminosities ( $M_V \lesssim -21.5$  mag) and large stellar velocity dispersions ( $\sigma \gtrsim 200$  km s $^{-1}$ ; see Dullo 2014; Dullo et al. 2023). We therefore include these galaxies in the comparison plots, while excluding

them from our primary core-Sérsic sample and from the baseline regression fits involving  $R_b$ .

In order to construct the  $M - \sigma$  relations, we used a sample of 121 dynamically determined SMBH masses from van den Bosch (2016, see their Table 2), excluding those in common with Dullo & Graham (2014), Dullo (2019), Dullo et al. (2021) and Dullo et al. (2023a). The majority ( $\sim 94\%$ ) of these galaxies are Sérsic galaxies, while a small fraction ( $\sim 6\%$ ), with  $M_{\text{BH}} \gtrsim 2 \times 10^9 M_\odot$  and  $\sigma \gtrsim 280$  km s $^{-1}$ , may be core-Sérsic galaxies with  $R_b < 0.5$  kpc.

Central stellar velocity dispersions ( $\sigma$ ) for the sample galaxies were primarily obtained from HyperLeda<sup>2</sup> (Paturel et al. 2003). For the BCGs, when HyperLeda  $\sigma$  values are not available, we adopt those from Lauer

<sup>2</sup><http://atlas.obs-hp.fr/hyperleda/>

**Table 1.** Core-Sérsic galaxies with directly measured black hole masses.

Galaxy	$D$	$\sigma$	$R_b$	$\log (M_{\text{BH}}/M_{\odot})$
	(Mpc)	(km s $^{-1}$ )	(kpc)	
(1)	(2)	(3)	(4)	(5)
IC 1459	30.9 [1]	296	0.108 [1]	$9.45^{+0.14}_{-0.24}$ [1]
NGC 0315	67.0 [14]	304	0.266 [14]	$9.49^{+0.14}_{-0.24}$ [2]
NGC 0584	19.6 [4]	198	0.021 [4]	$8.15^{+0.13}_{-0.19}$ [3]
NGC 1399	19.4 [4]	342	0.202 [4]	$9.07^{+0.7}_{-0.46}$ [4]
NGC 1407	28.1 [1]	266	0.276 [1]	$9.65^{+0.08}_{-0.04}$ [1]
NGC 1550	51.6 [1]	300	0.300 [1]	$9.57^{+0.05}_{-0.05}$ [1]
NGC 1600	66.0 [5]	331	0.650 [5]	$10.23^{+0.04}_{-0.04}$ [5]
NGC 3091	51.3 [1]	311	0.169 [1]	$9.56^{+0.01}_{-0.03}$ [1]
NGC 3379	10.3 [4]	209	0.102 [4]	$8.60^{+0.10}_{-0.13}$ [4]
NGC 3608	22.3 [4]	192	0.024 [4]	$8.30^{+0.19}_{-0.16}$ [4]
NGC 3640	26.3 [4]	191	0.005 [4]	$7.89^{+0.14}_{-0.24}$ [3]
NGC 3665	32.1 [14]	237	0.049 [14]	$8.73^{+0.14}_{-0.24}$ [6]
NGC 3706	45.2 [4]	259	0.024 [4]	$8.77^{+0.14}_{-0.24}$ [7]
NGC 3842	91.0 [4]	314	0.315 [4]	$9.98^{+0.12}_{-0.14}$ [4]
NGC 4261	31.6 [1]	297	0.198 [1]	$8.72^{+0.08}_{-0.10}$ [1]
NGC 4291	25.5 [4]	285	0.036 [4]	$8.52^{+0.11}_{-0.62}$ [4]
NGC 4374	18.5 [1]	278	0.139 [1]	$8.96^{+0.05}_{-0.04}$ [1]
NGC 4382	17.9 [4]	176	0.024 [4]	$7.98^{+0.05}_{-0.04}$ [8]
NGC 4472	15.8 [4]	294	0.108 [4]	$9.36^{+0.04}_{-0.02}$ [1]
NGC 4486	23.0 [5]	323	0.640 [5]	$9.76^{+0.03}_{-0.03}$ [5]
NGC 4552	14.9 [4]	253	0.017 [4]	$8.67^{+0.04}_{-0.05}$ [4]
NGC 4649	16.4 [4]	335	0.241 [4]	$9.67^{+0.08}_{-0.10}$ [4]
NGC 4889	96.6 [5]	347	0.860 [5]	$10.30^{+0.25}_{-0.62}$ [5]
NGC 5328	64.1 [1]	316	0.271 [1]	$9.67^{+0.08}_{-0.23}$ [1]
NGC 5516	58.4 [1]	309	0.178 [1]	$9.52^{+0.03}_{-0.04}$ [1]
NGC 5419	59.9 [4]	344	0.416 [4]	$10.04^{+0.03}_{-0.04}$ [9]
NGC 5813	31.3 [4]	237	0.051 [4]	$8.83^{+0.04}_{-0.05}$ [4]
NGC 6086	133.0 [1]	320	0.357 [1]	$9.56^{+0.17}_{-0.16}$ [1]
NGC 7619	51.5 [4]	317	0.109 [4]	$9.36^{+0.06}_{-0.12}$ [10]
NGC 7768	112.8 [1]	289	0.164 [1]	$9.11^{+0.14}_{-0.16}$ [1]
NGC 708 <sup>+</sup>	68.5 [11]	222 [11]	0.750 [11]	$10.00^{+0.12}_{-0.12}$ [11]
4C+37.11 <sup>+</sup>	246.9 [12]	332 [12]	1.603 [12]	$10.45^{+0.12}_{-0.12}$ [12]
Holm 15A <sup>+</sup>	252.8 [13]	346 [13]	2.840 [13]	$10.60^{+0.08}_{-0.10}$ [13]

Note. Col. (1) galaxy name. Col. (2) distance ( $D$ ). Col. (3) central velocity dispersion ( $\sigma$ ) are taken from HyperLeda (Paturel et al. 2003). Col. (4) core-Sérsic break radius ( $R_b$ ). Col. (5) SMBH mass adjusted to our distance. The subscript ‘+’ indicates galaxies that are not in our primary core-Sérsic galaxy sample (see the text for details). Sources: [1]=Rusli et al. (2013a); [2]=Pilawa et al. (2025); [3]= Thater et al. (2019); [4]=Dullo & Graham (2014, and references therein); [5]=Dullo (2019, and references therein); [6]=Onishi et al. (2017); [7]=Gültekin et al. (2014); [8]= Gültekin et al. (2011); [9]=Neureiter et al. (2023); [10]=Rusli et al. (2013b); [11]=de Nicola et al. (2024); [12]=Surti et al. (2024); [13]=Mehrgan et al. (2019); [14]=Dullo et al. (2023a).

**Table 2.** Core-Sérsic galaxies with predicted black hole masses.

Galaxy	$D$	$\sigma$	$R_b$	$M_V$
	(Mpc)	(km s $^{-1}$ )	(kpc)	(mag)
(1)	(2)	(3)	(4)	(5)
N0410	72.4	300	0.178	$-20.72 \pm 0.13$ [1]
N0507	63.7	292	0.102	$-22.56 \pm 0.27$ [2]
N0741	72.3	287	0.267	$-23.39 \pm 0.18$ [2]
N0777	68.8	324	0.208	$-20.68 \pm 0.22$ [1]
N1016	88.1	288	0.204	$-23.31 \pm 0.22$ [2]
N1167	68.0	217	0.045	$-19.72 \pm 0.27$ [1]
N2300	25.7	266	0.070	$-21.33 \pm 0.20$ [2]
N2832	105.0	327	0.483	$-24.58 \pm 0.23$ [1]
N3348	41.8	236	0.066	$-21.31 \pm 0.24$ [1]
N3613	31.7	220	0.038	$-21.39 \pm 0.34$ [1]
N4073	85.3	268	0.090	$-23.42 \pm 0.37$ [2]
N4278	15.6	237	0.052	$-20.91 \pm 0.27$ [2]
N4365	19.9	250	0.127	$-22.02 \pm 0.28$ [2]
N4406	16.7	231	0.061	$-22.31 \pm 0.12$ [2]
N4472	15.8	282	0.108	$-22.68 \pm 0.33$ [2]
N4589	21.4	219	0.027	$-21.04 \pm 0.24$ [2]
N4874	106.4	272	1.630	$-21.85 \pm 0.21$ [3]
N4914	70.8	225	0.035	$-20.93 \pm 0.25$ [1]
N5061	32.6	188	0.034	$-22.46 \pm 0.21$ [2]
N5322	27.0	230	0.054	$-21.77 \pm 0.24$ [2]
N5557	46.4	259	0.051	$-22.39 \pm 0.32$ [2]
N5631	29.3	168	0.006	$-20.85 \pm 0.19$ [1]
N5982	41.8	239	0.051	$-22.08 \pm 0.27$ [2]
N6166	130.4	300	2.110	$-24.62 \pm 0.25$ [3]
N6849	80.5	202	0.069	$-22.51 \pm 0.27$ [2]
N6876	54.3	233	0.119	$-23.51 \pm 0.19$ [2]
4C+74.13	925.3	239	2.240	$-24.12 \pm 0.20$ [3]
A0119BCG	185.7	283	0.670	$-24.51 \pm 0.21$ [3]
A0168BCG <sup>†</sup>	187.8 [4]	253	0.071	$-22.34 \pm 0.19$
A0189BCG <sup>†</sup>	116.7 [4]	212	0.108	$-22.55 \pm 0.17$
A0295BCG <sup>†</sup>	185.0 [4]	258	0.477	$-22.98 \pm 0.23$
A0419BCG <sup>†</sup>	136.5 [4]	189	0.139	$-22.38 \pm 0.22$

Note. Col. (1) galaxy name. Col. (2) distance ( $D$ ). Col. (3) central velocity dispersion ( $\sigma$ ) are from HyperLeda. For the BCGs, when HyperLeda  $\sigma$  values are not available, we use those from Lauer et al. (2014). Col. (4) core-Sérsic break radius ( $R_b$ ). Col. (5)  $V$ -band spheroid absolute magnitude ( $M_V$ ). The core-Sérsic break radii and  $V$ -band absolute spheroid magnitudes were measured from PSF-convolved core-Sérsic fits to the galaxies’ high-resolution HST surface brightness profiles (Dullo & Graham 2014; Dullo 2019; Dullo et al. 2023a). A ‘†’ indicates galaxies modeled in this work using HST WFPC2 light profiles. Sources for  $D$ ,  $R_b$  and  $M_V$  are: [1]=Dullo et al. (2023a); [2]=Dullo & Graham (2014); [3]=Dullo (2019); [4]=Laine et al. (2003); [5]=Dullo et al. (2017).

**Table 2.** – continued.

Galaxy	$D$ (Mpc)	$\sigma$ (km s <sup>-1</sup> )	$R_b$ (kpc)	$M_V$ (mag)
(1)	(2)	(3)	(4)	(5)
A0496BCG <sup>†</sup>	143.0 [4]	290	0.427	-23.78 ± 0.17
A0912BCG <sup>†</sup>	154.0 [4]	207	0.156	-22.62 ± 0.23
A1228BCG <sup>†</sup>	133.6 [4]	277	0.187	-22.88 ± 0.20
A1836BCG <sup>†</sup>	171.0 [4]	331	0.249	-23.61 ± 0.20
A1983BCG <sup>†</sup>	154.1 [4]	304	0.209	-22.95 ± 0.19
A2029BCG	363.0	386	4.200	-23.80 ± 0.23 [5]
A2147BCG	153.4	280	1.280	-23.61 ± 0.19 [3]
A2261BCG	958.8	387	3.333	-24.54 ± 0.21
A3376BCG <sup>†</sup>	208.0 [4]	319	1.551	-23.62 ± 0.25
A3395BCG <sup>†</sup>	217.0 [4]	287	0.341	-24.42 ± 0.19
A3528BCG <sup>†</sup>	246.0 [4]	364	0.641	-23.21 ± 0.18
A3556BCG <sup>†</sup>	218.0 [4]	347	0.383	-24.10 ± 0.25
A3558BCG	204.9	282	1.300	-25.40 ± 0.23 [3]
A3562BCG	213.3	263	0.640	-23.42 ± 0.26 [3]
A3571BCG	169.0	313	1.330	-23.35 ± 0.20 [3]
A3716BCG	246.0	275	0.497	-23.35 ± 0.21 [3]
A4059BCG <sup>†</sup>	214.0 [4]	289	0.853	-23.64 ± 0.25

et al. (2014). We assume a 10% uncertainty on  $\sigma$  when deriving the black hole scaling relations (Section 4).

### 2.1. Predicted black hole masses for core-Sérsic galaxies

To better investigate the black hole scaling relations, we use the velocity dispersion ( $\sigma$ ) and our  $V$ -band spheroid absolute magnitude ( $M_V$ ) for 49 (35 normal-core plus 14 large-core) galaxies (see Table 2) to predict their black hole masses. We made use of the [Graham & Scott \(2013, their Table 3\)](#) non-barred  $M_{\text{BH}} - \sigma$  relation to predict the  $\sigma$ -based SMBH masses. The  $L$ -based SMBH masses were predicted using the near-linear [Graham & Scott \(2013, their Table 3\)](#)  $B$ -band core-Sérsic  $M_{\text{BH}} - L$  relation transformed here into the  $V$ -band using total dust corrected  $B - V$  galaxy color from HyperLeda. We also use our  $M_{\text{BH}} - R_b$  relation to predict black hole masses for the 14 large-core galaxies in our sample with no directly measured black hole masses (Table 3).

## 3. REGRESSION ANALYSIS

To derive the black hole scaling relations (Table 4), we performed linear regressions using the Bivariate Correlated Errors and intrinsic Scatter (BCES) code ([Akritas & Bershady 1996](#)) and the Bayesian linear regression routine (LINMIX\_ERR, [Kelly 2007](#)). The fitted BCES bisector regressions, based on the python module by [Nem-](#)

**Table 3.** Large-core galaxy data

Galaxy	Predicted black hole masses		
	$(\sigma\text{-based})$	$(L\text{-based})$	$(R_b\text{-based})$
(1)	(2)	(3)	(4)
NGC 4874	8.91 <sup>+0.42</sup> <sub>-0.42</sub>	9.02 <sup>+0.34</sup> <sub>-0.34</sub>	10.50 <sup>+0.45</sup> <sub>-0.45</sub>
NGC 6166	9.19 <sup>+0.43</sup> <sub>-0.43</sub>	10.50 <sup>+0.47</sup> <sub>-0.47</sub>	10.60 <sup>+0.46</sup> <sub>-0.46</sub>
4C+74.13	8.68 <sup>+0.41</sup> <sub>-0.41</sub>	10.23 <sup>+0.41</sup> <sub>-0.41</sub>	10.65 <sup>+0.46</sup> <sub>-0.46</sub>
A0119	9.06 <sup>+0.43</sup> <sub>-0.43</sub>	10.45 <sup>+0.46</sup> <sub>-0.46</sub>	10.12 <sup>+0.42</sup> <sub>-0.42</sub>
A2029	9.74 <sup>+0.47</sup> <sub>-0.47</sub>	10.06 <sup>+0.40</sup> <sub>-0.40</sub>	10.97 <sup>+0.44</sup> <sub>-0.44</sub>
A2147	9.03 <sup>+0.42</sup> <sub>-0.42</sub>	9.95 <sup>+0.41</sup> <sub>-0.41</sub>	10.38 <sup>+0.44</sup> <sub>-0.44</sub>
A2261	9.75 <sup>+0.48</sup> <sub>-0.48</sub>	10.46 <sup>+0.47</sup> <sub>-0.47</sub>	10.80 <sup>+0.45</sup> <sub>-0.45</sub>
A3376	9.32 <sup>+0.41</sup> <sub>-0.41</sub>	9.96 <sup>+0.47</sup> <sub>-0.47</sub>	10.49 <sup>+0.43</sup> <sub>-0.43</sub>
A3528	9.61 <sup>+0.44</sup> <sub>-0.44</sub>	9.74 <sup>+0.47</sup> <sub>-0.47</sub>	10.09 <sup>+0.41</sup> <sub>-0.41</sub>
A3558	9.05 <sup>+0.41</sup> <sub>-0.41</sub>	10.92 <sup>+0.54</sup> <sub>-0.54</sub>	10.40 <sup>+0.44</sup> <sub>-0.44</sub>
A3562	8.90 <sup>+0.41</sup> <sub>-0.41</sub>	9.85 <sup>+0.39</sup> <sub>-0.39</sub>	10.09 <sup>+0.42</sup> <sub>-0.42</sub>
A3571	9.28 <sup>+0.44</sup> <sub>-0.44</sub>	9.81 <sup>+0.39</sup> <sub>-0.39</sub>	10.41 <sup>+0.43</sup> <sub>-0.43</sub>
A3716	8.99 <sup>+0.42</sup> <sub>-0.42</sub>	9.81 <sup>+0.54</sup> <sub>-0.54</sub>	9.91 <sup>+0.42</sup> <sub>-0.42</sub>
A4059	9.10 <sup>+0.42</sup> <sub>-0.42</sub>	9.97 <sup>+0.54</sup> <sub>-0.54</sub>	10.19 <sup>+0.43</sup> <sub>-0.43</sub>
Dynamically determined black hole masses			
Galaxy	$\log(M_{\text{BH}}/M_{\odot})$	Galaxy	$\log(M_{\text{BH}}/M_{\odot})$
NGC 708	10.00 <sup>+0.12</sup> <sub>-0.12</sub>	NGC 4889	10.30 <sup>+0.25</sup> <sub>-0.62</sub>
NGC 1600	10.23 <sup>+0.04</sup> <sub>-0.04</sub>	4C+37.11	10.45 <sup>+0.12</sup> <sub>-0.12</sub>
NGC 4486	9.76 <sup>+0.03</sup> <sub>-0.03</sub>	Holm 15A	10.60 <sup>+0.08</sup> <sub>-0.10</sub>

Note. Col. (1) galaxy name. Cols. (2–4) SMBH and UMBH masses were predicted using the  $M_{\text{BH}} - \sigma$ ,  $M_{\text{BH}} - L_{\text{sph}}$ , and  $M_{\text{BH}} - R_b$  relations, respectively, for our sample of 14 large-core galaxies without dynamically determined SMBH mass measurements (Section 2.1). The lower part of the table lists six galaxies<sup>a</sup> with dynamically determined black hole masses reported to be large-core galaxies in the literature. (see the text for details).

<sup>a</sup>We note that three of these six galaxies with directly measured BH masses (NGC 1600, NGC 4486, and NGC 4889) are already included in Table 1.

[men et al. \(2012\)](#), are symmetrical and bisect the forward ( $Y|X$ ) and inverse ( $X|Y$ ) lines. Both the BCES and LINMIX\_ERR methods allow us to account for errors in the variables under consideration (e.g., [Dullo et al. 2020, 2021](#)). We note that a forward regression ( $Y|X$ ) tend to yield a shallower slope than an inverse regression,  $X|Y$  ([Feigelson & Babu 1992](#)). To address the ‘theorist’s question’, i.e., the intrinsic correlations between two quantities, symmetrical regressions are generally preferred when the ‘dependent’ and ‘independent’ variables are not clearly defined ([Novak et al. 2006](#)). The BCES bisector regressions are presented throughout this paper (Table 4). Nevertheless, our symmetric BCES relations are consistent within the errors with the forward ( $Y|X$ ) regressions obtained with BCES and LINMIX

Table 4. Black Hole Scaling Relations

Relation	BCES fit	$\Delta_{\text{rms}}$	$\epsilon$	$r_s/P$	$r_p/P$	Sample
<b>Dynamically measured SMBH masses only</b>						
<b>Core-Sérsic galaxies</b>						
$M_{\text{BH}} - R_b$	$\log\left(\frac{M_{\text{BH}}}{M_{\odot}}\right) = (1.16 \pm 0.10)\log\left(\frac{R_b}{250 \text{ pc}}\right) + (9.56 \pm 0.05)$	0.28	$0.27 \pm 0.05$	$0.91/5.6 \times 10^{-12}$	$0.90/1.1 \times 10^{-11}$	30 [a]
$M_{\text{BH}} - \sigma$	$\log\left(\frac{M_{\text{BH}}}{M_{\odot}}\right) = (9.20 \pm 1.53)\log\left(\frac{\sigma}{300 \text{ km s}^{-1}}\right) + (9.51 \pm 0.07)$	0.40	$0.20 \pm 0.09$	$0.85/1.8 \times 10^{-9}$	$0.86/9.9 \times 10^{-10}$	30 [a]
<b>Including 4C+37.11, Holm 15A, and NGC 708</b>						
$M_{\text{BH}} - R_b$	$\log\left(\frac{M_{\text{BH}}}{M_{\odot}}\right) = (1.15 \pm 0.08)\log\left(\frac{R_b}{250 \text{ pc}}\right) + (9.55 \pm 0.05)$	0.27	$0.27 \pm 0.05$	$0.93/2.0 \times 10^{-14}$	$0.92/5.1 \times 10^{-14}$	33 [b]
$M_{\text{BH}} - \sigma$	$\log\left(\frac{M_{\text{BH}}}{M_{\odot}}\right) = (10.22 \pm 1.69)\log\left(\frac{\sigma}{300 \text{ km s}^{-1}}\right) + (9.61 \pm 0.09)$	0.51	$0.31 \pm 0.09$	$0.79/3.4 \times 10^{-8}$	$0.79/4.7 \times 10^{-8}$	33 [b]
<b>Sérsic plus Core-Sérsic galaxies</b>						
$M_{\text{BH}} - \sigma$	$\log\left(\frac{M_{\text{BH}}}{M_{\odot}}\right) = (4.95 \pm 0.29)\log\left(\frac{\sigma}{200 \text{ km s}^{-1}}\right) + (8.35 \pm 0.04)$	0.46	$0.39 \pm 0.03$	$0.85/2.1 \times 10^{-43}$	$0.85/1.2 \times 10^{-43}$	148 [c]
$M_{\text{BH}} - \sigma$	$\log\left(\frac{M_{\text{BH}}}{M_{\odot}}\right) = (5.10 \pm 0.29)\log\left(\frac{\sigma}{200 \text{ km s}^{-1}}\right) + (8.37 \pm 0.04)$	0.47	$0.39 \pm 0.03$	$0.86/1.1 \times 10^{-45}$	$0.85/4.0 \times 10^{-44}$	151 [d]
<b>Including 4C+37.11, Holm 15A, and NGC 708</b>						
$M_{\text{BH}} - \sigma$	$\log\left(\frac{M_{\text{BH}}}{M_{\odot}}\right) = (5.28 \pm 0.31)\log\left(\frac{\sigma}{200 \text{ km s}^{-1}}\right) + (8.39 \pm 0.04)$	0.50	$0.42 \pm 0.04$	$0.86/1.4 \times 10^{-46}$	$0.85/1.0 \times 10^{-44}$	154 [e]
<b>Including predicted SMBH masses</b>						
<b>Core-Sérsic galaxies</b>						
$M_{\text{BH}} - \sigma$	$\log\left(\frac{M_{\text{BH}}}{M_{\odot}}\right) = (11.21 \pm 1.58)\log\left(\frac{\sigma}{300 \text{ km s}^{-1}}\right) + (9.86 \pm 0.11)$	0.72	$0.34 \pm 0.12$	$0.56/1.6 \times 10^{-4}$	$0.66/1.0 \times 10^{-6}$	44 [f]
<b>Including 4C+37.11, Holm 15A, and NGC 708</b>						
$M_{\text{BH}} - \sigma$	$\log\left(\frac{M_{\text{BH}}}{M_{\odot}}\right) = (11.00 \pm 1.26)\log\left(\frac{\sigma}{300 \text{ km s}^{-1}}\right) + (9.90 \pm 0.10)$	0.72	$0.41 \pm 0.11$	$0.57/7.8 \times 10^{-5}$	$0.65/2.5 \times 10^{-6}$	47 [g]
<b>Sérsic plus Core-Sérsic galaxies</b>						
$M_{\text{BH}} - \sigma$	$\log\left(\frac{M_{\text{BH}}}{M_{\odot}}\right) = (5.87 \pm 0.37)\log\left(\frac{\sigma}{200 \text{ km s}^{-1}}\right) + (8.45 \pm 0.05)$	0.58	$0.44 \pm 0.04$	$0.85/6.1 \times 10^{-47}$	$0.82/7.1 \times 10^{-42}$	165 [h]
<b>Including 4C+37.11, Holm 15A, and NGC 708</b>						
$M_{\text{BH}} - \sigma$	$\log\left(\frac{M_{\text{BH}}}{M_{\odot}}\right) = (5.99 \pm 0.37)\log\left(\frac{\sigma}{200 \text{ km s}^{-1}}\right) + (8.47 \pm 0.05)$	0.60	$0.46 \pm 0.04$	$0.86/4.1 \times 10^{-48}$	$0.83/1.1 \times 10^{-43}$	168 [i]

Note—The different columns represent: the BH scaling relations, rms scatter in the vertical  $\log M_{\text{BH}}$  direction ( $\Delta_{\text{rms}}$ ), intrinsic scatter from the Bayesian LINMIX fits ( $\epsilon$ ), and the Spearman and Pearson correlation coefficients ( $r_s$  and  $r_p$ , respectively) and the associated probabilities. For scaling relations including predicted SMBH masses, the SMBH masses were predicted from the  $M_{\text{BH}} - R_b$  relation, see Table 3. Definitions of samples ([a]–[i]) are presented in Table 5.

**Table 5.** Definition of Galaxy Samples Used in Table 4

Sample	Description
[a]	30 core-Sérsic galaxies with dynamically determined SMBH masses: 15 normal-core galaxies from <a href="#">Dullo &amp; Graham (2014)</a> , 10 normal-core ellipticals from <a href="#">Rusli et al. (2013a)</a> , 3 large-core ellipticals from <a href="#">Dullo (2019)</a> , and 2 normal-core galaxies from <a href="#">Dullo et al. (2023a)</a> .
[b]	33 core-Sérsic galaxies: the 30 galaxies in sample [a] plus 4C+37.11 ( <a href="#">Surti et al. 2024</a> ), Holm 15A ( <a href="#">Mehrgan et al. 2019</a> ), and NGC 708 ( <a href="#">de Nicola et al. 2024</a> ).
[c]	148 non-large-core galaxies: 27 normal-core galaxies from sample [a] plus 121 galaxies with dynamically measured SMBH masses from <a href="#">van den Bosch (2016)</a> not in common with <a href="#">Rusli et al. (2013a)</a> ; <a href="#">Dullo &amp; Graham (2014)</a> ; <a href="#">Dullo (2019)</a> ; <a href="#">Dullo et al. (2023a)</a> .
[d]	151 galaxies: the 148 galaxies in sample [c] plus 3 large-core ellipticals from <a href="#">Dullo (2019)</a> .
[e]	154 galaxies: the 151 galaxies in sample [d] plus 4C+37.11, Holm 15A and NGC 708.
[f]	44 core-Sérsic galaxies: the 30 galaxies in sample [a] plus 14 large-core galaxies with SMBH masses predicted from the $M_{\text{BH}} - R_b$ relation (Table 3).
[g]	47 core-Sérsic galaxies: the 44 galaxies in sample [f] plus 4C+37.11, Holm 15A, and NGC 708.
[h]	165 galaxies: the 151 galaxies in sample [d] plus 14 large-core galaxies with predicted SMBH masses from Table 3.
[i]	168 galaxies: the 154 galaxies in sample [e] plus 14 large-core galaxies with predicted SMBH masses from Table 3.

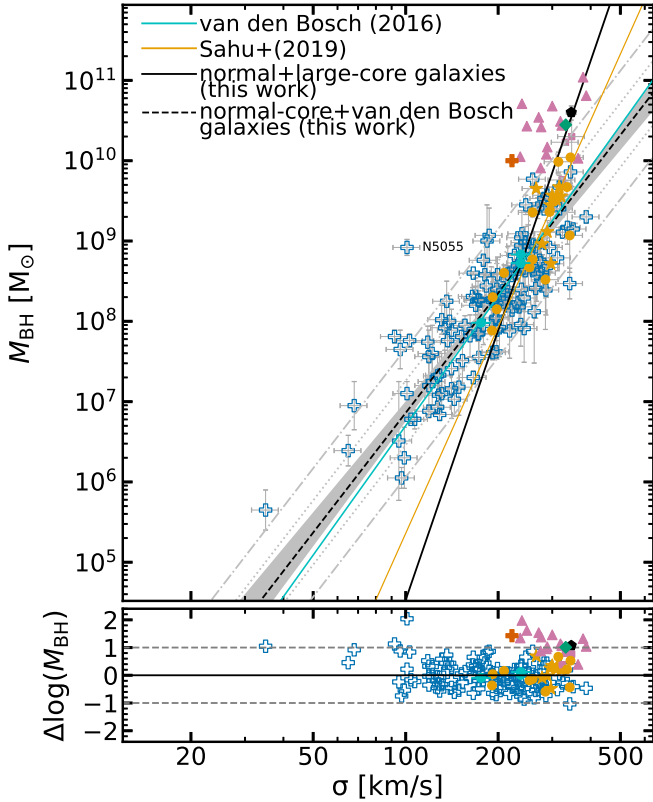


**Figure 2.** SMBH mass ( $M_{\text{BH}}$ ) plotted as a function of central velocity dispersion ( $\sigma$ ). Similar to Fig. 1(b) but here we also show the 121 galaxies with dynamically determined SMBH masses from van den Bosch (2016) that are not in common with Rusli et al. (2013a); Dullo & Graham (2014); Dullo (2019), open crosses. In addition, we show 14 large-core galaxies with SMBH masses predicted using the  $M_{\text{BH}} - R_{\text{b}}$  relation (filled purple triangles; Table 2). The black dashed line represents our symmetric BCES bisector fit to the  $(M_{\text{BH}}, \sigma)$  data for the composite sample of 148 non-(large-core) galaxies with directly measured BH masses—121 galaxies from van den Bosch (2016), 17 normal-core galaxies (Dullo & Graham 2014) and 10 normal-core ellipticals (Rusli et al. 2013a). The shaded region shows the  $1\sigma$  uncertainty for the fit. The dotted and dashed-dotted lines show one and two times the measured vertical rms scatter in the log  $M_{\text{BH}}$  direction ( $\Delta_{\text{rms}} = 0.46$  dex), respectively. The lower panel shows the residual profile about the fit. The solid black line is the BCES bisector fit to the 44 core-Sersic galaxies (i.e., 30 with directly measured  $M_{\text{BH}}$  plus 14 large-cores with  $M_{\text{BH}}$  predicted using the  $M_{\text{BH}} - R_{\text{b}}$  relation). The solid cyan line indicates the  $M_{\text{BH}} - \sigma$  relation found by van den Bosch (2016) for their full sample of 230 galaxies, while the solid orange line is the core-Sersic  $M_{\text{BH}} - \sigma$  relation reported by Sahu et al. (2019).

(see Table 4 and Appendix A1). Additionally, we re-analyzed the data using the symmetric orthogonal BCES regressions and obtained consistent results.

We quantify the strength of the correlations using the Spearman and Pearson correlation coefficients and the associated  $p$ -values, for which the null hypothesis that the two data sets are uncorrelated is true. The intrinsic scatter from our LINMIX regression fits to the  $(M_{\text{BH}}, R_{\text{b}})$  and  $(M_{\text{BH}}, \sigma)$  data sets (e.g., Dullo et al. 2020),  $\epsilon$ , as well as the vertical root-mean-square (rms) scatter in the log  $M_{\text{BH}}$  directions ( $\Delta_{\text{rms}}$ ), are presented in Table 4.

## 4. RESULTS

### 4.1. $M_{\text{BH}} - R_{\text{b}}$ and $M_{\text{BH}} - \sigma$ relations for core-Sersic galaxies

Fig. 1 plots the  $M_{\text{BH}} - R_{\text{b}}$  and  $M_{\text{BH}} - \sigma$  relations for our sample of 30 core-Sersic galaxies with directly measured SMBH masses. The intrinsic scatter in the  $M_{\text{BH}} - R_{\text{b}}$  relation is  $\epsilon \sim 0.27 \pm 0.05$ . The correlation between  $M_{\text{BH}}$  and  $R_{\text{b}}$  has a total rms scatter in log  $M_{\text{BH}}$  direction of  $\Delta \sim 0.28$  dex, Spearman correlation coefficient ( $r_{\text{s}}$ )/ $p$ -value of  $0.91/5.6 \times 10^{-12}$  and Pearson correlation coefficient ( $r_{\text{p}}$ )/ $p$ -value of  $0.90/1.1 \times 10^{-11}$ . In contrast, the core-Sersic  $M_{\text{BH}} - \sigma$  relation constructed using the same sample (Fig. 1) has  $\epsilon \sim 0.25 \pm 0.05$ ,  $\Delta \sim 0.40$  dex,  $r_{\text{s}}$ / $p$ -value  $0.85/1.8 \times 10^{-9}$  and  $r_{\text{p}}$ / $p$ -value  $0.86/9.9 \times 10^{-10}$  (Table 4).

The slope of the updated  $M_{\text{BH}} - R_{\text{b}}$  relation ( $1.16 \pm 0.10$ ) is in good agreement with those reported in previous studies, including Dullo & Graham (2012, their Eqs. 11 and 12 with an average slope of  $1.29 \pm 0.33$ ), Rusli et al. (2013a,  $1.09 \pm 0.20$ ), Dullo & Graham (2014,  $1.25 \pm 0.25$ ) and Dullo et al. (2021,  $1.20 \pm 0.25$ ).

Using a sample of 33 core-Sersic galaxies, i.e., including three galaxies recently reported to host UMBHs and large cores (4C+37.11, Surti et al. 2024, Holm 15A, Mehrgan et al. 2019, and NGC 708, de Nicola et al. 2024), we obtain a consistent relation ( $M_{\text{BH}} \propto R_{\text{b}}^{1.15 \pm 0.08}$ ); see Tables 3 and 4. This relation has a total rms scatter in log  $M_{\text{BH}}$  direction of  $\Delta \sim 0.27$  dex, a Spearman correlation coefficient ( $r_{\text{s}}$ )/ $p$ -value of  $0.93/2.0 \times 10^{-14}$  and a Pearson correlation coefficient ( $r_{\text{p}}$ )/ $p$ -value of  $0.92/5.1 \times 10^{-14}$ . The corresponding core-Sersic  $M_{\text{BH}} - \sigma$  relation (Fig. 1) has  $\epsilon \sim 0.31 \pm 0.09$ ,  $\Delta \sim 0.51$  dex,  $r_{\text{s}}$ / $p$ -value  $0.79/3.4 \times 10^{-8}$  and  $r_{\text{p}}$ / $p$ -value  $0.79/4.7 \times 10^{-8}$  (Table 4).

Our sample consists of a total of six galaxies which host UMBHs  $M_{\text{BH}} \gtrsim 10^{10} M_{\odot}$ , representing  $\sim 18\%$  of all the core-Sersic galaxies with measured  $M_{\text{BH}}$  to date. Fig. 1 shows that the large-core galaxies (purple boxes, black hexagon, green diamond and orange cross) follow the log-linear  $M_{\text{BH}} - R_{\text{b}}$  relation traced by the relatively less massive, normal-core population (filled orange circles, cyan disk symbol and filled orange stars), see Tables 1, 3 and 4. The large break radii of all the six large-

core galaxies with measured  $M_{\text{BH}}$  (4C+37.11, NGC 708, NGC 1600, NGC 4486, NGC 4889 and Holm 15A) are in good agreement with the galaxies' large black hole masses (Fig. 1).

We compare the  $M_{\text{BH}} - R_{\text{b}}$  and  $M_{\text{BH}} - \sigma$  relations constructed using the same sample (see Table 4). We find that the tight  $M_{\text{BH}} - R_{\text{b}}$  relation exhibits  $\sim 30\text{--}47\%$  less scatter in  $\log M_{\text{BH}}$  than the core-Sérsic  $M_{\text{BH}} - \sigma$  relation, albeit the two relations exhibit a similar level of intrinsic scatter ( $\epsilon \sim 0.26 \pm 0.06$ ).

#### 4.2. The $M_{\text{BH}} - \sigma$ relation

In order to investigate the upturn tendency of the  $M_{\text{BH}} - \sigma$  relation at high  $\sigma$ , we derive its slopes by dividing our sample into Sérsic, normal-core and large-core galaxies. Fig. 2 shows the best-fitting BCES bisector regression for the sample of 148 galaxies (dashed line): 121 galaxies from van den Bosch (2016) (most which are Sérsic galaxies) and 27 normal-core galaxies (Table 2). The shaded region represents the  $1\sigma$  uncertainty of the fit. We find that non-(large-core) (i.e., Sérsic and normal-core) galaxies define a single log-linear  $M_{\text{BH}} - \sigma$  relation with a slope of  $4.95 \pm 0.29$ ,  $\epsilon \sim 0.39$  dex and  $\Delta_{\text{rms}} \sim 0.46$  dex in the  $\log M_{\text{BH}}$ , consistent with previous studies (Graham & Scott 2013; Savorgnan & Graham 2015; van den Bosch 2016; Krajnović et al. 2018; Dullo et al. 2020, 2021). When the 27 normal-core galaxies are excluded from the regression analysis, the BCES bisector  $M_{\text{BH}} - \sigma$  relation for the 121 galaxies remains similar, with a slope of  $\sim 4.66 \pm 0.29$  and an intercept of  $\sim -2.39 \pm 0.67$ .

While the core-Sérsic  $M_{\text{BH}} - \sigma$  relation for our sample of 30 core-Sérsic galaxies with directly measured SMBH masses (Fig. 1) has a significantly steeper slope of  $9.20 \pm 1.53$  and an intercept of  $\sim -13.28 \pm 3.79$ , we did not find evidence for a marked division between Sérsic and normal-core galaxies, albeit see Sahu et al. (2019). We have compared the relative quality of a single unified  $M_{\text{BH}} - \sigma$  relation with separate Sérsic and normal-core relations using the Akaike Information Criterion (AIC, Akaike 1974) and Bayesian Information Criterion (BIC, Schwarz 1978).

$$\text{AIC} = 2k - 2 \ln(\mathcal{L}), \quad (1)$$

$$\text{BIC} = k \ln(n) - 2 \ln(\mathcal{L}), \quad (2)$$

and a variation of the AIC, AICc can be written as

$$\text{AICc} = \text{AIC} + \frac{2k(k+1)}{n-k-1} \quad (3)$$

where  $\mathcal{L}$  is the maximum value of the likelihood function for the model,  $k$  is the number of free parameters of the model and  $n$  is the sample size.

We use two approaches to derive the AIC and BIC for the single power-law and broken models: one based on our bisector BCES fits, and the other on the LINMIX fits. For the bisector BCES-based models (Table 4), we approximate the model evidence using the residual sum of squares under the assumption of Gaussian residuals. For the LINMIX-based models (see Appendix), we use the LINMIX intrinsic scatter (Table 4) as part of the Gaussian likelihood to compute the AIC and BIC. In both cases, we assumed normally distributed residuals. We find  $\text{AIC}_{\text{bc}, \text{single}} - \text{AIC}_{\text{bc}, \text{broken}} (= \Delta \text{AIC}_{\text{bc}}) \sim 1.8$  and  $\text{AIC}_{\text{linmix}, \text{single}} - \text{AIC}_{\text{linmix}, \text{broken}} (= \Delta \text{AIC}_{\text{linmix}}) \sim 1.6$ , which indicate that the additional complexity of the broken model is not warranted by the data. Furthermore, the BIC strongly favors the simpler single relation ( $\Delta \text{BIC}_{\text{bc}} \sim -4$  and  $\Delta \text{BIC}_{\text{linmix}} \sim -7$ ). Overall, our results suggest that the  $(M_{\text{BH}}, \sigma)$  dataset for the non-(large-core) galaxies is better described with a single power-law rather than a broken, i.e. two separate power-laws<sup>3</sup>.

Our sample consists of three large-core galaxies with directly measured SMBH masses (purple boxes), see Figs. 1, 2 and Table 2. We find that these six galaxies are *offset upward* by  $\sim (1-2) \times \sigma_s$  from the  $M_{\text{BH}} - \sigma$  sequence traced by Sérsic and normal-core galaxies (Fig. 2). We adopt that  $1\sigma_s$  equals the intrinsic scatter  $\epsilon = 0.39$  dex.

In Figs. 1 and 2, we also show 4C+37.11 (green diamond), Holm 15A (black hexagon), and NGC 708 (orange cross), all hosting host UMBHs. We find that that 4C+37.11, Holm 15A, and NGC 708 lie 1.01, 1.15 and 1.43 dex above the non-(large-core)  $M_{\text{BH}} - \sigma$  relation, respectively, and are thus offset upward by  $(2.6-3.7) \times \sigma_s$  (Fig. 2).

While the inclusion of the six large-core galaxies (4C+37.11, NGC 708, NGC 1600, NGC 4486, NGC 4889 and Holm 15A) in the regression analyses slightly steepens the non-(large-core)  $M_{\text{BH}} - \sigma$  relation (Table 4, slope =  $5.28 \pm 0.31$ ), the two slopes are consistent within  $1\sigma$ .

#### 4.3. The $M_{\text{BH}} - \sigma$ relation including predicted SMBH masses

In this section, we investigate the  $M_{\text{BH}} - \sigma$  relation by including 14 large-core galaxies with BH masses predicted using the tight  $M_{\text{BH}} - R_{\text{b}}$  relation (Fig. 2,

<sup>3</sup>For the BCES-based single and broken models,  $k = 2$  and  $k = 4$ , respectively. In contrast,  $k = 3$  and  $k = 6$  for the LINMIX-based single and broken models, respectively, because the intrinsic scatter is included as an additional parameter in the Gaussian likelihood function.

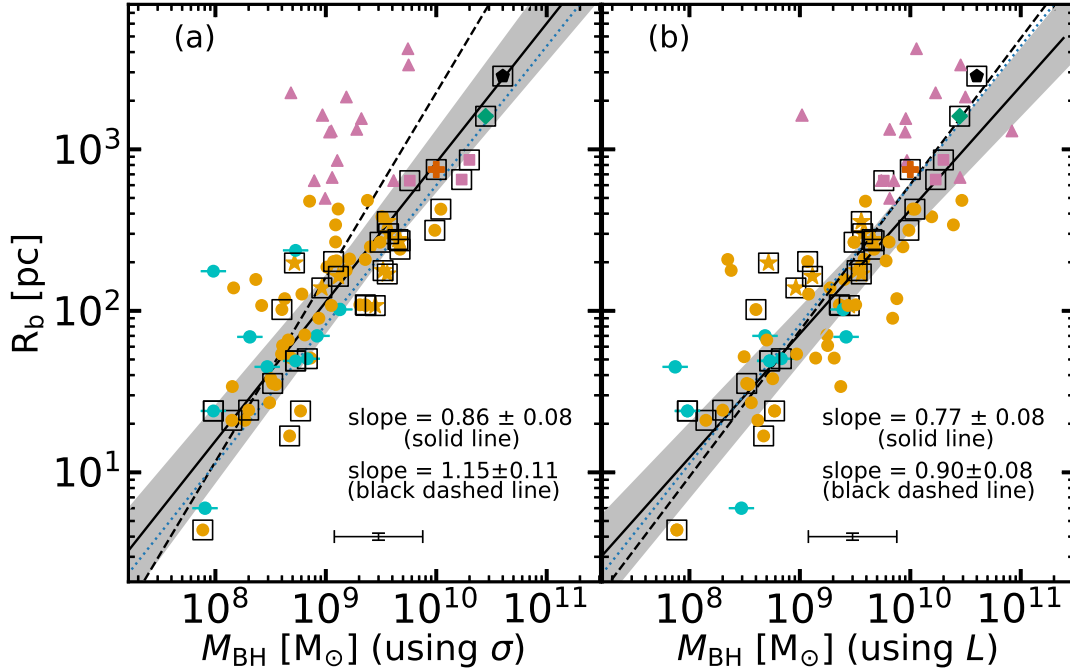


**Figure 3.** Relationship between  $R_b$  and  $M_{\text{BH}}$  for 79 core-Sérsic galaxies. Similar to Fig. 1(a), but here, besides the 30 core-Sérsic galaxies with directly measured  $M_{\text{BH}}$ , we include 49 (35 normal-core plus 14 large-core) core-Sérsic galaxies with SMBH masses that are predicted using the [Graham & Scott \(2013\)](#) non-barred  $M_{\text{BH}} - \sigma$  relation (a) and their  $B$ -band core-Sérsic  $M_{\text{BH}} - L$  relation (b). Symbolic representations are as in Fig. 2. All core-Sérsic galaxies with directly measured  $M_{\text{BH}}$  are enclosed in boxes. The blue dotted lines represent the  $R_b - M_{\text{BH}}$  relation for our full sample of 30 core-Sérsic galaxies with measured SMBH masses (see Fig. 1a and Table 2). The black solid lines are the symmetric OLS bisector regressions for 65 core-Sérsic galaxies (excluding the 14 large-core galaxies with predicted SMBH masses) and the shaded regions show the associated  $1\sigma$  uncertainties. The black dashed lines are the symmetric OLS bisector fits to the full sample of 79 core-Sérsic galaxies. For reference, we also show 4C+37.11 (diamond), Holm 15A (hexagon), and NGC 708 (cross).

purple triangles, Section 2.1), and Table 4). The inclusion of these large-core galaxies significantly steepens the  $M_{\text{BH}} - \sigma$  relation (Fig. 2, the solid black line with a slope of  $11.21 \pm 1.58$ ). We find that large-core galaxies with  $(M_{\text{BH}} - R_b)$ -based BH masses deviate upward by  $(1 - 5) \times \sigma_s$  from the  $M_{\text{BH}} - \sigma$  relation traced by non-(large-core) galaxies with directly measured BH masses (Fig. 2). Excluding large-core galaxies, the most deviant outlier in the  $M_{\text{BH}} - \sigma$  diagram is the spiral galaxy NGC 5055, see also [Dullo et al. \(2020\)](#).

#### 4.4. The $R_b - M_{\text{BH}}$ relation

Fig. 3 plots the core-Sérsic break radius against black hole mass for our full sample of 79 core-Sérsic galaxies. The 30 core-Sérsic galaxies with directly measured black hole masses are enclosed in boxes. For the 49 (35 normal-core plus 14 large-core) galaxies with no direct SMBH measurements, the predicted black hole masses based on  $\sigma$  and  $L_{\text{sph}}$  are shown in Figs. 3a and 3b, respectively. Excluding the 14 large-core galaxies with  $\sigma$ -based SMBH masses (see Table 2), we fit the ordinary least squares (OLS) bisector regression by [Feigelson & Babu \(1992\)](#) to the  $(R_b, M_{\text{BH}})$

data of our 65 core-Sérsic galaxies (Fig. 3a). This fit yields  $\log(R_b/\text{pc}) = (0.86 \pm 0.08) \log(M_{\text{BH}}/10^9) + (2.06 \pm 0.05)$ . This relation (black solid line) is consistent, within the errors, with that shown in Fig. 1(a) based on core-Sérsic galaxies with measured  $M_{\text{BH}}$  (Fig. 3, blue dotted lines), although the latter is vertically shifted by 0.14 dex.

In contrast, Figs. 3a shows that fitting the OLS bisector to the full sample of 79 core-Sérsic galaxies results in a steeper slope of  $\sim 1.14 \pm 0.11$  and a larger intercept of  $\sim 2.21 \pm 0.10$ . The discrepancy is attributed to the non-large-core (i.e., Sérsic + normal-core)  $M_{\text{BH}} - \sigma$  relation, which tend to underestimate SMBH masses in giant spheroids with large depleted cores (see also [Bernardi et al. 2007](#); [Lauer et al. 2007](#); [McConnell et al. 2011, 2012](#); [Volonteri & Ciotti 2013](#); [Mezcua et al. 2018](#)).

In Fig. 3(b), we find that the non-large-core  $R_b - M_{\text{BH}}$  relation from our OLS bisector fit to 65 core-Sérsic galaxies (i.e., excluding the 14 large-core galaxies with  $L_{\text{sph}}$ -based SMBH masses, Table 2) has a slope of  $\sim 0.77 \pm 0.07$  and an intercept  $\sim 1.86 \pm 0.05$  in fair agree-

ment with those for the full core-Sérsic population (slope  $\sim 0.90 \pm 0.08$  and intercept  $\sim 1.89 \pm 0.09$ ).

## 5. DRY MERGERS AND THE HIGH-MASS UPTURN

As noted above, the most massive galaxies appear to host BHs that are overmassive relative to expectations from their central velocity dispersions, resulting in an upturn in the  $M_{\text{BH}}-\sigma$  relation (e.g., Lauer et al. 2007; Hlavacek-Larrondo et al. 2012; Mezcua et al. 2018; Dullo 2019; Dullo et al. 2021; Sasseville et al. 2025). Simulations by Boylan-Kolchin et al. (2006) have predicted that merger orbits become increasingly radial at the highest galaxy masses. In such dry (nearly parabolic) mergers, orbital energy is converted into internal energy of the remnant, causing the galaxy to grow in size roughly in proportion to its stellar mass. Under the virial theorem and energy conservation, the velocity dispersion is expected to remain largely unchanged during these events (e.g., Nipoti et al. 2003; Ciotti et al. 2007; Bezanon et al. 2009; Volonteri & Ciotti 2013; Bernardi et al. 2011). Large-core spheroids are thought to have experienced several ( $\sim 6-10$ ) successive major dry mergers (Dullo 2019), which add stars, increase BH mass and enlarge depleted core, while leaving  $\sigma$  approximately constant.

Systematic uncertainties in BH mass measurements may also contribute to the observed upturn. Dynamically measured BH masses in brightest cluster galaxies (BCGs) may be biased high owing to limitations in data quality, assumptions in dynamical modeling, or the treatment of the dark matter halo (e.g., McConnell et al. 2011; Thater et al. 2022). In addition, structural non-homology in the most massive galaxies may introduce additional scatter or systematic deviations from the standard BH scaling relations at the high-mass end (e.g., Frigo & Balcells 2017).

## 6. CONCLUSIONS

Partially depleted cores in luminous, core-Sérsic galaxies are thought to form through the transfer of orbital angular momentum from inspiraling binary SMBHs to stars near the galaxy center, thereby scouring the core. The core-Sérsic model describes the underlying spheroidal light distributions of these galaxies, allowing the size of the depleted core to be quantified via the break radius ( $R_{\text{b}}$ ). We use a large sample of 151 galaxies with dynamically determined SMBH masses ( $M_{\text{BH}}$ ), to investigate the correlations between  $M_{\text{BH}}$  and central velocity dispersion ( $\sigma$ ) and for a subsample of 30 core-Sérsic galaxies, between  $M_{\text{BH}}$  and  $R_{\text{b}}$ . We expand the sample of core-Sérsic galaxies with directly

measured SMBH masses from 24 (Dullo et al. 2021) to 30, constituting a 25% increase, and those with predicted SMBH masses from 27 (Dullo et al. 2021) to 49, an  $\sim 82\%$  increase. Our final sample comprises 79 core-Sérsic galaxies, identified through detailed modeling of the galaxies' high-resolution *HST* surface brightness profiles. Our main results are summarized as follows:

1) We find a tight correlation between SMBH mass and core size,  $M_{\text{BH}} \propto R_{\text{b}}^{1.16 \pm 0.10}$ , which holds across the full mass range of core-Sérsic, including both normal-core and large-core spheroids. This updated relation has Spearman and Pearson correlation coefficients of  $\sim 0.92$ , and an intrinsic scatter of  $0.27 \pm 0.07$  dex. Including three galaxies recently reported to host UMBHs and large cores, namely 4C+37.11 (Surti et al. 2024), Holm 15A (Mehrgan et al. 2019), and NGC 708 (de Nicola et al. 2024), does not alter the relation ( $M_{\text{BH}} \propto R_{\text{b}}^{1.15 \pm 0.08}$ ), although the measurement of the break radii for the galaxies is less secure.

2) The  $M_{\text{BH}} - R_{\text{b}}$  relation has a vertical rms scatter in the  $\log M_{\text{BH}}$  of  $\Delta_{\text{rms}} \sim 0.28$  dex. It is significantly stronger than the core-Sérsic  $M_{\text{BH}} - \sigma$  relation constructed using the same sample, exhibiting  $\sim 30-47\%$  less scatter in the  $\log M_{\text{BH}}$ . The latter has Spearman and Pearson correlation coefficients of  $\sim 0.79 - 0.85$  and a vertical rms scatter of  $\Delta_{\text{rms}} \sim 0.45 \pm 0.05$  dex.

3) Dividing the sample into Sérsic, normal-core and large-core galaxies, we find a single, updated log-linear  $M_{\text{BH}} - \sigma$  relation for Sérsic and normal-core galaxies with a slope of  $4.95 \pm 0.29$ ,  $\epsilon \sim 0.39$  dex and  $\Delta_{\text{rms}} \sim 0.46$  dex. Including large-core galaxies with directly measured BH masses tend to steepen the relation slightly to  $5.28 \pm 0.31$ , albeit the slopes are consistent within the errors. While core-Sérsic galaxies alone define a much steeper relation with a slope of  $\sim 9.20 \pm 1.53$ , our results suggest that Sérsic and normal-core galaxies are better described by a common log-linear  $M_{\text{BH}}-\sigma$  relation, rather than a broken relation.

4) Supermassive and ultramassive black hole masses in large-core galaxies, whether directly measured or predicted using the  $M_{\text{BH}} - R_{\text{b}}$  relation, are systematically underestimated by the  $M_{\text{BH}} - \sigma$  relation defined by Sérsic plus normal-core galaxies. Three galaxies recently reported to host ultramassive black holes—4C+37.11 (Surti et al. 2024), Holm 15A (Mehrgan et al. 2019), and NGC 708 (de Nicola et al. 2024)—are offset by 1.01, 1.15 and 1.43 dex above the non-(large-core)  $M_{\text{BH}} - \sigma$  relation, respectively. Overall, we find that large-core galaxies with directly measured BH masses are offset upward typically by  $(1 - 4) \times \sigma_{\text{s}}$  from the  $M_{\text{BH}} - \sigma$  sequence traced by Sérsic+normal-core galax-

**Table A1.** Linear Regression Analysis with BCES

Relation	BCES (Y X) fit	Sample
(1)	(2)	(3)
<b>Dynamically measured SMBH masses only</b>		
<b>Core-Sérsic galaxies</b>		
$M_{\text{BH}} - R_{\text{b}}$	$\log\left(\frac{M_{\text{BH}}}{M_{\odot}}\right) = (1.08 \pm 0.10)\log\left(\frac{R_{\text{b}}}{250 \text{ pc}}\right) + (9.53 \pm 0.06)$	30 [a]
$M_{\text{BH}} - \sigma$	$\log\left(\frac{M_{\text{BH}}}{M_{\odot}}\right) = (9.79 \pm 17.21)\log\left(\frac{\sigma}{300 \text{ km s}^{-1}}\right) + (9.53 \pm 0.11)$	30 [a]
<b>Including 4C+37.11, Holm 15A, and NGC 708</b>		
$M_{\text{BH}} - R_{\text{b}}$	$\log\left(\frac{M_{\text{BH}}}{M_{\odot}}\right) = (1.06 \pm 0.08)\log\left(\frac{R_{\text{b}}}{250 \text{ pc}}\right) + (9.51 \pm 0.05)$	33 [b]
$M_{\text{BH}} - \sigma$	$\log\left(\frac{M_{\text{BH}}}{M_{\odot}}\right) = (10.40 \pm 13.47)\log\left(\frac{\sigma}{300 \text{ km s}^{-1}}\right) + (9.61 \pm 0.16)$	33 [b]
<b>Sérsic plus Core-Sérsic galaxies</b>		
$M_{\text{BH}} - \sigma$	$\log\left(\frac{M_{\text{BH}}}{M_{\odot}}\right) = (4.57 \pm 0.31)\log\left(\frac{\sigma}{200 \text{ km s}^{-1}}\right) + (8.35 \pm 0.04)$	148 [c]
$M_{\text{BH}} - \sigma$	$\log\left(\frac{M_{\text{BH}}}{M_{\odot}}\right) = (4.69 \pm 0.32)\log\left(\frac{\sigma}{200 \text{ km s}^{-1}}\right) + (8.37 \pm 0.04)$	151 [d]
$M_{\text{BH}} - \sigma$	$\log\left(\frac{M_{\text{BH}}}{M_{\odot}}\right) = (4.83 \pm 0.33)\log\left(\frac{\sigma}{200 \text{ km s}^{-1}}\right) + (8.39 \pm 0.04)$	154 [e]
<b>Including predicted SMBH masses</b>		
<b>Core-Sérsic galaxies</b>		
$M_{\text{BH}} - \sigma$	$\log\left(\frac{M_{\text{BH}}}{M_{\odot}}\right) = (9.70 \pm 1.77)\log\left(\frac{\sigma}{300 \text{ km s}^{-1}}\right) + (9.82 \pm 0.10)$	44 [e]
<b>Including 4C+37.11, Holm 15A, and NGC 708</b>		
$M_{\text{BH}} - \sigma$	$\log\left(\frac{M_{\text{BH}}}{M_{\odot}}\right) = (9.34 \pm 1.68)\log\left(\frac{\sigma}{300 \text{ km s}^{-1}}\right) + (9.85 \pm 0.09)$	47 [f]
<b>Sérsic plus Core-Sérsic galaxies</b>		
$M_{\text{BH}} - \sigma$	$\log\left(\frac{M_{\text{BH}}}{M_{\odot}}\right) = (5.26 \pm 0.36)\log\left(\frac{\sigma}{200 \text{ km s}^{-1}}\right) + (8.46 \pm 0.05)$	165 [g]
$M_{\text{BH}} - \sigma$	$\log\left(\frac{M_{\text{BH}}}{M_{\odot}}\right) = (5.36 \pm 0.36)\log\left(\frac{\sigma}{200 \text{ km s}^{-1}}\right) + (8.48 \pm 0.05)$	168 [i]

NOTE—Similar to Table 4, but shown here are the forward BCES (Y|X) regressions.

ies, where  $\sigma_{\text{s}}$  denotes the intrinsic scatter (0.39 dex). This behavior is consistent with a galaxy formation history dominated by late-time dry mergers, which add stars, increase BH mass, while leaving  $\sigma$  largely unchanged. Our results are consistent with studies of giant ellipticals and BCGs showing saturation of  $\sigma$  at highest luminosities. As such, the high-mass upturn of large-core galaxies in the  $M_{\text{BH}} - \sigma$  diagram and the flattening of the  $\sigma - L_V$  relation at  $M_V \lesssim -23.5$  mag (Dullo 2019) are internally consistent.

## ACKNOWLEDGMENTS

We thank the referee for a timely and constructive report that improved this manuscript. B.D. is grateful to Jason Aufdenberg for useful comments.

*Facilities:* HST (WFPC2, ACS, NICMOS, WFC3)

This work has made use of NUMPY (van der Walt et al. 2011), MATPLOTLIB (Hunter 2007) and ASTROPY, a community-developed core PYTHON package for Astronomy (Astropy Collaboration et al. 2013, 2018), ASTROQUERY (Ginsburg et al. 2019) CUBEHELIX (Green 2011), (Kluyver et al. 2016), SCIPY (Virtanen et al. 2020), and of TOPCAT (i.e. ‘Tool for Operations on Catalogues And Tables’, Taylor 2005) and ChatGPT (OpenAI 2023, 2025).

## APPENDIX

### A1. BCES AND LINMIX Y|X REGRESSIONS

Table A1 presents the BH scaling relations derived from our forward (Y|X) regression fits using BCES, whereas Table A2 presents those obtained from (Y|X) regressions using LINMIX.

**Table A2.** Linear Regression Analysis with LINMIX

Relation	LINMIX (Y X) fit	Sample
(1)	(2)	(3)
<b>Dynamically measured SMBH masses only</b>		
<b>Core-Sérsic galaxies</b>		
$M_{\text{BH}} - R_{\text{b}}$	$\log\left(\frac{M_{\text{BH}}}{M_{\odot}}\right) = (1.04 \pm 0.11)\log\left(\frac{R_{\text{b}}}{250 \text{ pc}}\right) + (9.53 \pm 0.06)$	30 [a]
$M_{\text{BH}} - \sigma$	$\log\left(\frac{M_{\text{BH}}}{M_{\odot}}\right) = (8.23 \pm 1.19)\log\left(\frac{\sigma}{300 \text{ km s}^{-1}}\right) + (9.50 \pm 0.09)$	30 [a]
<b>Including 4C+37.11, Holm 15A, and NGC 708</b>		
$M_{\text{BH}} - R_{\text{b}}$	$\log\left(\frac{M_{\text{BH}}}{M_{\odot}}\right) = (1.01 \pm 0.09)\log\left(\frac{R_{\text{b}}}{250 \text{ pc}}\right) + (9.52 \pm 0.06)$	33 [b]
$M_{\text{BH}} - \sigma$	$\log\left(\frac{M_{\text{BH}}}{M_{\odot}}\right) = (9.15 \pm 1.41)\log\left(\frac{\sigma}{300 \text{ km s}^{-1}}\right) + (9.60 \pm 0.10)$	33 [b]
<b>Sérsic plus Core-Sérsic galaxies</b>		
$M_{\text{BH}} - \sigma$	$\log\left(\frac{M_{\text{BH}}}{M_{\odot}}\right) = (4.59 \pm 0.25)\log\left(\frac{\sigma}{200 \text{ km s}^{-1}}\right) + (8.38 \pm 0.04)$	148 [c]
$M_{\text{BH}} - \sigma$	$\log\left(\frac{M_{\text{BH}}}{M_{\odot}}\right) = (4.70 \pm 0.25)\log\left(\frac{\sigma}{200 \text{ km s}^{-1}}\right) + (8.39 \pm 0.04)$	151 [d]
$M_{\text{BH}} - \sigma$	$\log\left(\frac{M_{\text{BH}}}{M_{\odot}}\right) = (4.84 \pm 0.26)\log\left(\frac{\sigma}{200 \text{ km s}^{-1}}\right) + (8.41 \pm 0.04)$	154 [e]
<b>Including predicted SMBH masses</b>		
<b>Core-Sérsic galaxies</b>		
$M_{\text{BH}} - \sigma$	$\log\left(\frac{M_{\text{BH}}}{M_{\odot}}\right) = (9.20 \pm 1.51)\log\left(\frac{\sigma}{300 \text{ km s}^{-1}}\right) + (9.71 \pm 0.10)$	44 [e]
<b>Including 4C+37.11, Holm 15A, and NGC 708</b>		
$M_{\text{BH}} - \sigma$	$\log\left(\frac{M_{\text{BH}}}{M_{\odot}}\right) = (9.10 \pm 1.55)\log\left(\frac{\sigma}{300 \text{ km s}^{-1}}\right) + (9.77 \pm 0.10)$	47 [f]
<b>Sérsic plus Core-Sérsic galaxies</b>		
$M_{\text{BH}} - \sigma$	$\log\left(\frac{M_{\text{BH}}}{M_{\odot}}\right) = (5.03 \pm 0.25)\log\left(\frac{\sigma}{200 \text{ km s}^{-1}}\right) + (8.45 \pm 0.04)$	165 [g]
$M_{\text{BH}} - \sigma$	$\log\left(\frac{M_{\text{BH}}}{M_{\odot}}\right) = (5.16 \pm 0.26)\log\left(\frac{\sigma}{200 \text{ km s}^{-1}}\right) + (8.47 \pm 0.04)$	168 [i]

NOTE—Similar to Table 4, but shown here are the forward LINMIX (Y|X) regressions.

## REFERENCES

- Akaike, H. 1974, *IEEE Transactions on Automatic Control*, 19, 716, doi: [10.1109/TAC.1974.1100705](https://doi.org/10.1109/TAC.1974.1100705)
- Akritas, M. G., & Bershady, M. A. 1996, *ApJ*, 470, 706, doi: [10.1086/177901](https://doi.org/10.1086/177901)
- Astropy Collaboration, Robitaille, T. P., Tollerud, E. J., et al. 2013, *A&A*, 558, A33, doi: [10.1051/0004-6361/201322068](https://doi.org/10.1051/0004-6361/201322068)
- Astropy Collaboration, Price-Whelan, A. M., Sipőcz, B. M., et al. 2018, *AJ*, 156, 123, doi: [10.3847/1538-3881/aabc4f](https://doi.org/10.3847/1538-3881/aabc4f)
- Begelman, M. C., Blandford, R. D., & Rees, M. J. 1980, *Nature*, 287, 307, doi: [10.1038/287307a0](https://doi.org/10.1038/287307a0)
- Bernardi, M., Hyde, J. B., Sheth, R. K., Miller, C. J., & Nichol, R. C. 2007, *AJ*, 133, 1741, doi: [10.1086/511783](https://doi.org/10.1086/511783)
- Bernardi, M., Roche, N., Shankar, F., & Sheth, R. K. 2011, *MNRAS*, 412, 684, doi: [10.1111/j.1365-2966.2010.17984.x](https://doi.org/10.1111/j.1365-2966.2010.17984.x)
- Bezanson, R., van Dokkum, P. G., Tal, T., et al. 2009, *ApJ*, 697, 1290, doi: [10.1088/0004-637X/697/2/1290](https://doi.org/10.1088/0004-637X/697/2/1290)
- Boylan-Kolchin, M., Ma, C.-P., & Quataert, E. 2006, *MNRAS*, 369, 1081, doi: [10.1111/j.1365-2966.2006.10379.x](https://doi.org/10.1111/j.1365-2966.2006.10379.x)
- Carollo, C. M., Franx, M., Illingworth, G. D., & Forbes, D. A. 1997, *ApJ*, 481, 710, doi: [10.1086/304060](https://doi.org/10.1086/304060)
- Ciotti, L., Lanzoni, B., & Volonteri, M. 2007, *ApJ*, 658, 65, doi: [10.1086/510773](https://doi.org/10.1086/510773)
- de Nicola, S., Thomas, J., Saglia, R. P., et al. 2024, *MNRAS*, 530, 1035, doi: [10.1093/mnras/stae806](https://doi.org/10.1093/mnras/stae806)
- Dullo, B. T. 2019, *ApJ*, 886, 80, doi: [10.3847/1538-4357/ab4d4f](https://doi.org/10.3847/1538-4357/ab4d4f)
- Dullo, B. T., Bouquin, A. Y. K., Gil de Paz, A., Knapen, J. H., & Gorgas, J. 2020, *ApJ*, 898, 83, doi: [10.3847/1538-4357/ab9dff](https://doi.org/10.3847/1538-4357/ab9dff)
- Dullo, B. T., Gil de Paz, A., & Knapen, J. H. 2021, *ApJ*, 908, 134, doi: [10.3847/1538-4357/abceae](https://doi.org/10.3847/1538-4357/abceae)
- Dullo, B. T., & Graham, A. W. 2012, *ApJ*, 755, 163, doi: [10.1088/0004-637X/755/2/163](https://doi.org/10.1088/0004-637X/755/2/163)
- . 2014, *MNRAS*, 444, 2700, doi: [10.1093/mnras/stu1590](https://doi.org/10.1093/mnras/stu1590)
- . 2015, *ApJ*, 798, 55, doi: [10.1088/0004-637X/798/1/55](https://doi.org/10.1088/0004-637X/798/1/55)
- Dullo, B. T., Graham, A. W., & Knapen, J. H. 2017, *MNRAS*, 471, 2321, doi: [10.1093/mnras/stx1635](https://doi.org/10.1093/mnras/stx1635)
- Dullo, B. T., Knapen, J. H., Beswick, R. J., et al. 2023a, *A&A*, 675, A105, doi: [10.1051/0004-6361/202345913](https://doi.org/10.1051/0004-6361/202345913)

- . 2023b, *MNRAS*, 522, 3412, doi: [10.1093/mnras/stad1122](https://doi.org/10.1093/mnras/stad1122)
- Dullo, B. T., Knapen, J. H., Baldi, R. D., et al. 2024, *MNRAS*, 532, 4729, doi: [10.1093/mnras/stae1732](https://doi.org/10.1093/mnras/stae1732)
- Ebisuzaki, T., Makino, J., & Okumura, S. K. 1991, *Nature*, 354, 212, doi: [10.1038/354212a0](https://doi.org/10.1038/354212a0)
- Faber, S. M., & Jackson, R. E. 1976, *ApJ*, 204, 668, doi: [10.1086/154215](https://doi.org/10.1086/154215)
- Feigelson, E. D., & Babu, G. J. 1992, *ApJ*, 397, 55, doi: [10.1086/171766](https://doi.org/10.1086/171766)
- Ferrarese, L., & Ford, H. 2005, *SSRv*, 116, 523, doi: [10.1007/s11214-005-3947-6](https://doi.org/10.1007/s11214-005-3947-6)
- Ferrarese, L., & Merritt, D. 2000, *ApJL*, 539, L9, doi: [10.1086/312838](https://doi.org/10.1086/312838)
- Frigo, M., & Balcells, M. 2017, *MNRAS*, 469, 2184, doi: [10.1093/mnras/stx875](https://doi.org/10.1093/mnras/stx875)
- Gebhardt, K., Bender, R., Bower, G., et al. 2000, *ApJL*, 539, L13, doi: [10.1086/312840](https://doi.org/10.1086/312840)
- Ginsburg, A., Sipőcz, B. M., Brasseur, C. E., et al. 2019, *AJ*, 157, 98, doi: [10.3847/1538-3881/aafc33](https://doi.org/10.3847/1538-3881/aafc33)
- Graham, A. W., & Scott, N. 2013, *ApJ*, 764, 151, doi: [10.1088/0004-637X/764/2/151](https://doi.org/10.1088/0004-637X/764/2/151)
- Green, D. A. 2011, *Bulletin of the Astronomical Society of India*, 39, 289. <https://arxiv.org/abs/1108.5083>
- Gualandris, A., & Merritt, D. 2012, *ApJ*, 744, 74, doi: [10.1088/0004-637X/744/1/74](https://doi.org/10.1088/0004-637X/744/1/74)
- Gültekin, K., Gebhardt, K., Kormendy, J., et al. 2014, *ApJ*, 781, 112, doi: [10.1088/0004-637X/781/2/112](https://doi.org/10.1088/0004-637X/781/2/112)
- Gültekin, K., Richstone, D. O., Gebhardt, K., et al. 2011, *ApJ*, 741, 38, doi: [10.1088/0004-637X/741/1/38](https://doi.org/10.1088/0004-637X/741/1/38)
- Håring, N., & Rix, H.-W. 2004, *ApJL*, 604, L89, doi: [10.1086/383567](https://doi.org/10.1086/383567)
- Held, E. V., de Zeeuw, T., Mould, J., & Picard, A. 1992, *AJ*, 103, 851, doi: [10.1086/116106](https://doi.org/10.1086/116106)
- Hlavacek-Larrondo, J., Fabian, A. C., Edge, A. C., & Hogan, M. T. 2012, *MNRAS*, 424, 224, doi: [10.1111/j.1365-2966.2012.21187.x](https://doi.org/10.1111/j.1365-2966.2012.21187.x)
- Hunter, J. D. 2007, *Computing in Science & Engineering*, 9, 90, doi: [10.1109/MCSE.2007.55](https://doi.org/10.1109/MCSE.2007.55)
- Kelly, B. C. 2007, *ApJ*, 665, 1489, doi: [10.1086/519947](https://doi.org/10.1086/519947)
- Khan, F. M., Holley-Bockelmann, K., Berczik, P., & Just, A. 2013, *ApJ*, 773, 100, doi: [10.1088/0004-637X/773/2/100](https://doi.org/10.1088/0004-637X/773/2/100)
- Khochfar, S., & Burkert, A. 2001, *ApJ*, 561, 517, doi: [10.1086/323382](https://doi.org/10.1086/323382)
- Kluyver, T., Ragan-Kelley, B., Pérez, F., et al. 2016, in *Positioning and Power in Academic Publishing: Players, Agents and Agendas*, ed. F. Loizides & B. Schmidt, Amsterdam: IOS Press, 87 – 90
- Kormendy, J., & Bender, R. 2013, *ApJL*, 769, L5, doi: [10.1088/2041-8205/769/1/L5](https://doi.org/10.1088/2041-8205/769/1/L5)
- Kormendy, J., & Richstone, D. 1995, *ARA&A*, 33, 581, doi: [10.1146/annurev.aa.33.090195.003053](https://doi.org/10.1146/annurev.aa.33.090195.003053)
- Krajnović, D., Cappellari, M., & McDermid, R. M. 2018, *MNRAS*, 473, 5237, doi: [10.1093/mnras/stx2704](https://doi.org/10.1093/mnras/stx2704)
- Laine, S., van der Marel, R. P., Lauer, T. R., et al. 2003, *AJ*, 125, 478, doi: [10.1086/345823](https://doi.org/10.1086/345823)
- Lauer, T. R., Postman, M., Strauss, M. A., Graves, G. J., & Chisari, N. E. 2014, *ApJ*, 797, 82, doi: [10.1088/0004-637X/797/2/82](https://doi.org/10.1088/0004-637X/797/2/82)
- Lauer, T. R., Faber, S. M., Richstone, D., et al. 2007, *ApJ*, 662, 808, doi: [10.1086/518223](https://doi.org/10.1086/518223)
- Magorrian, J., Tremaine, S., Richstone, D., et al. 1998, *AJ*, 115, 2285, doi: [10.1086/300353](https://doi.org/10.1086/300353)
- Malumuth, E. M., & Kirshner, R. P. 1981, *ApJ*, 251, 508, doi: [10.1086/159490](https://doi.org/10.1086/159490)
- Marconi, A., & Hunt, L. K. 2003, *ApJL*, 589, L21, doi: [10.1086/375804](https://doi.org/10.1086/375804)
- Matković, A., & Guzmán, R. 2005, *MNRAS*, 362, 289, doi: [10.1111/j.1365-2966.2005.09298.x](https://doi.org/10.1111/j.1365-2966.2005.09298.x)
- McConnell, N. J., & Ma, C.-P. 2013, *ApJ*, 764, 184, doi: [10.1088/0004-637X/764/2/184](https://doi.org/10.1088/0004-637X/764/2/184)
- McConnell, N. J., Ma, C.-P., Gebhardt, K., et al. 2011, *Nature*, 480, 215, doi: [10.1038/nature10636](https://doi.org/10.1038/nature10636)
- McConnell, N. J., Ma, C.-P., Murphy, J. D., et al. 2012, *ApJ*, 756, 179, doi: [10.1088/0004-637X/756/2/179](https://doi.org/10.1088/0004-637X/756/2/179)
- McLure, R. J., & Dunlop, J. S. 2002, *MNRAS*, 331, 795, doi: [10.1046/j.1365-8711.2002.05236.x](https://doi.org/10.1046/j.1365-8711.2002.05236.x)
- Mehrgan, K., Thomas, J., Saglia, R., et al. 2019, *ApJ*, 887, 195, doi: [10.3847/1538-4357/ab5856](https://doi.org/10.3847/1538-4357/ab5856)
- Merritt, D. 2006, *ApJ*, 648, 976, doi: [10.1086/506139](https://doi.org/10.1086/506139)
- Mezcua, M., Hlavacek-Larrondo, J., Lucey, J. R., et al. 2018, *MNRAS*, 474, 1342, doi: [10.1093/mnras/stx2812](https://doi.org/10.1093/mnras/stx2812)
- Milosavljević, M., & Merritt, D. 2001, *ApJ*, 563, 34, doi: [10.1086/323830](https://doi.org/10.1086/323830)
- Nasim, I., Gualandris, A., Read, J., et al. 2020, *MNRAS*, 497, 739, doi: [10.1093/mnras/staa1896](https://doi.org/10.1093/mnras/staa1896)
- Nemmen, R. S., Georganopoulos, M., Guiriec, S., et al. 2012, *Science*, 338, 1445, doi: [10.1126/science.1227416](https://doi.org/10.1126/science.1227416)
- Neureiter, B., Thomas, J., Rantala, A., et al. 2023, *ApJ*, 950, 15, doi: [10.3847/1538-4357/acffa](https://doi.org/10.3847/1538-4357/acffa)
- Nipoti, C., Londrillo, P., & Ciotti, L. 2003, *MNRAS*, 342, 501, doi: [10.1046/j.1365-8711.2003.06554.x](https://doi.org/10.1046/j.1365-8711.2003.06554.x)
- Novak, G. S., Faber, S. M., & Dekel, A. 2006, *ApJ*, 637, 96, doi: [10.1086/498333](https://doi.org/10.1086/498333)
- Oegerle, W. R., & Hoessel, J. G. 1991, *ApJ*, 375, 15, doi: [10.1086/170165](https://doi.org/10.1086/170165)
- Onishi, K., Iguchi, S., Davis, T. A., et al. 2017, *MNRAS*, 468, 4663, doi: [10.1093/mnras/stx631](https://doi.org/10.1093/mnras/stx631)

- OpenAI. 2023, ChatGPT (GPT-4), Accessed: 2023-03-15  
 —. 2025, ChatGPT (GPT-5), Accessed: 2025-03-15
- Patuarel, G., Petit, C., Prugniel, P., et al. 2003, *A&A*, 412, 45, doi: [10.1051/0004-6361:20031411](https://doi.org/10.1051/0004-6361:20031411)
- Pilawa, J., Liepold, E. R., Ma, C.-P., Walsh, J. L., & Greene, J. E. 2025, *ApJ*, 989, 98, doi: [10.3847/1538-4357/adee1e](https://doi.org/10.3847/1538-4357/adee1e)
- Rantala, A., Johansson, P. H., Naab, T., Thomas, J., & Frigo, M. 2018, *ApJ*, 864, 113, doi: [10.3847/1538-4357/aada47](https://doi.org/10.3847/1538-4357/aada47)
- Rusli, S. P., Erwin, P., Saglia, R. P., et al. 2013a, *AJ*, 146, 160, doi: [10.1088/0004-6256/146/6/160](https://doi.org/10.1088/0004-6256/146/6/160)
- Rusli, S. P., Thomas, J., Saglia, R. P., et al. 2013b, *AJ*, 146, 45, doi: [10.1088/0004-6256/146/3/45](https://doi.org/10.1088/0004-6256/146/3/45)
- Sahu, N., Graham, A. W., & Davis, B. L. 2019, *ApJ*, 887, 10, doi: [10.3847/1538-4357/ab50b7](https://doi.org/10.3847/1538-4357/ab50b7)
- Sasseville, G., Hlavacek-Larrondo, J., Berek, S. C., et al. 2025, *ApJ*, 978, 48, doi: [10.3847/1538-4357/ad93d4](https://doi.org/10.3847/1538-4357/ad93d4)
- Savognan, G. A. D., & Graham, A. W. 2015, *MNRAS*, 446, 2330, doi: [10.1093/mnras/stu2259](https://doi.org/10.1093/mnras/stu2259)
- Schwarz, G. 1978, *The Annals of Statistics*, 6, 461, doi: [10.1214/aos/1176344136](https://doi.org/10.1214/aos/1176344136)
- Sérsic, J. L. 1963, *Boletín de la Asociación Argentina de Astronomía La Plata Argentina*, 6, 41
- . 1968, *Atlas de Galaxias Australes (Córdoba, Argentina: Observatorio Astronómico)*
- Sheth, R. K., Bernardi, M., Schechter, P. L., et al. 2003, *ApJ*, 594, 225, doi: [10.1086/376794](https://doi.org/10.1086/376794)
- Surti, T., Romani, R. W., Scharwächter, J., Peck, A., & Taylor, G. B. 2024, *ApJ*, 960, 110, doi: [10.3847/1538-4357/ad14fa](https://doi.org/10.3847/1538-4357/ad14fa)
- Taylor, M. B. 2005, in *Astronomical Society of the Pacific Conference Series*, Vol. 347, *Astronomical Data Analysis Software and Systems XIV*, ed. P. Shopbell, M. Britton, & R. Ebert, 29
- Thater, S., Krajnović, D., Cappellari, M., et al. 2019, *A&A*, 625, A62, doi: [10.1051/0004-6361/201834808](https://doi.org/10.1051/0004-6361/201834808)
- Thater, S., Krajnović, D., Weilbacher, P. M., et al. 2022, *MNRAS*, 509, 5416, doi: [10.1093/mnras/stab3210](https://doi.org/10.1093/mnras/stab3210)
- Thomas, J., Ma, C.-P., McConnell, N. J., et al. 2016, *Nature*, 532, 340, doi: [10.1038/nature17197](https://doi.org/10.1038/nature17197)
- van den Bosch, R. C. E. 2016, *ApJ*, 831, 134, doi: [10.3847/0004-637X/831/2/134](https://doi.org/10.3847/0004-637X/831/2/134)
- van der Walt, S., Colbert, S. C., & Varoquaux, G. 2011, *Computing in Science and Engineering*, 13, 22, doi: [10.1109/MCSE.2011.37](https://doi.org/10.1109/MCSE.2011.37)
- Vasiliev, E., Antonini, F., & Merritt, D. 2015, *ApJ*, 810, 49, doi: [10.1088/0004-637X/810/1/49](https://doi.org/10.1088/0004-637X/810/1/49)
- Virtanen, P., Gommers, R., Oliphant, T. E., et al. 2020, *Nature Methods*, 17, 261, doi: [10.1038/s41592-019-0686-2](https://doi.org/10.1038/s41592-019-0686-2)
- Volonteri, M., & Ciotti, L. 2013, *ApJ*, 768, 29, doi: [10.1088/0004-637X/768/1/29](https://doi.org/10.1088/0004-637X/768/1/29)
- White, S. D. M., & Frenk, C. S. 1991, *ApJ*, 379, 52, doi: [10.1086/170483](https://doi.org/10.1086/170483)
- White, S. D. M., & Rees, M. J. 1978, *MNRAS*, 183, 341, doi: [10.1093/mnras/183.3.341](https://doi.org/10.1093/mnras/183.3.341)